NEURAL REGENERATION RESEARCH
www.nrronline.org

Research Article

Exacerbated VEGF up-regulation accompanies diabetes-aggravated hemorrhage in mice after experimental cerebral ischemia and delayed reperfusion

https://doi.org/10.4103/1673-5374.330612
Date of submission: April 16, 2021
Date of decision: May 19, 2021
Date of acceptance: June 11, 2021
Date of web publication: December 10, 2021

Angela Ka Wai Lai[1, #], Tsz Chung Ng[1, #], Victor Ka Lok Hung[2], Ka Cheung Tam[1], Chi Wai Cheung[2], Sookja Kim Chung[3], Amy Cheuk Yin Lo[1, *]

From the Contents

Graphical Abstract *Vascular endothelial growth factor (VEGF) and aggravated hemorrhage in diabetic stroke*

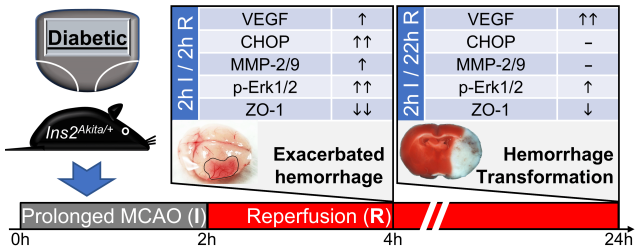

Abstract

Reperfusion therapy is the preferred treatment for ischemic stroke, but is hindered by its short treatment window, especially in patients with diabetes whose reperfusion after prolonged ischemia is often accompanied by exacerbated hemorrhage. The mechanisms underlying exacerbated hemorrhage are not fully understood. This study aimed to identify this mechanism by inducing prolonged 2-hour transient intraluminal middle cerebral artery occlusion in diabetic *Ins2*$^{Akita/+}$ mice to mimic patients with diabetes undergoing delayed mechanical thrombectomy. The results showed that at as early as 2 hours after reperfusion, *Ins2*$^{Akita/+}$ mice exhibited rapid development of neurological deficits, increased infarct and hemorrhagic transformation, together with exacerbated down-regulation of tight-junction protein ZO-1 and up-regulation of blood-brain barrier-disrupting matrix metallopeptidase 2 and matrix metallopeptidase 9 when compared with normoglycemic *Ins2*$^{+/+}$ mice. This indicated that diabetes led to the rapid compromise of vessel integrity immediately after reperfusion, and consequently earlier death and further aggravation of hemorrhagic transformation 22 hours after reperfusion. This observation was associated with earlier and stronger up-regulation of pro-angiogenic vascular endothelial growth factor (VEGF) and its downstream phospho-Erk1/2 at 2 hours after reperfusion, which was suggestive of premature angiogenesis induced by early VEGF up-regulation, resulting in rapid vessel disintegration in diabetic stroke. Endoplasmic reticulum stress-related pro-apoptotic C/EBP homologous protein was overexpressed in challenged *Ins2*$^{Akita/+}$ mice, which suggests that the exacerbated VEGF up-regulation may be caused by overwhelming endoplasmic reticulum stress under diabetic conditions. In conclusion, the results mimicked complications in patients with diabetes undergoing delayed mechanical thrombectomy, and diabetes-induced accelerated VEGF up-regulation is likely to underlie exacerbated hemorrhagic transformation. Thus, suppression of the VEGF pathway could be a potential approach to allow reperfusion therapy in patients with diabetic stroke beyond the current treatment window. Experiments were approved by the Committee on the Use of Live Animals in Teaching and Research of the University of Hong Kong [CULATR 3834-15 (approval date January 5, 2016); 3977-16 (approval date April 13, 2016); and 4666-18 (approval date March 29, 2018)].

Key Words: blood-brain barrier; brain injury; diabetes mellitus; hemorrhagic transformation; infarct; ischemia/reperfusion injury; middle cerebral artery occlusion; mouse model; stroke; vascular endothelial growth factor

Chinese Library Classification No. R453; R364; Q2

[1]Department of Ophthalmology, Li Ka Shing Faculty of Medicine, The University of Hong Kong, Hong Kong Special Administration Region, China; [2]Department of Anesthesiology, Laboratory and Clinical Research Institute for Pain, The University of Hong Kong, Hong Kong Special Administration Region, China; [3]Macau University of Science and Technology, Taipa, Macau Special Administration Region, China; School of Biomedical Sciences, The State Key Laboratory of Pharmaceutical Biotechnology, The University of Hong Kong, Hong Kong Special Administration Region, China
*Correspondence to: Amy Cheuk Yin Lo, PhD, amylo@hku.hk.
https://orcid.org/0000-0003-4239-6851 (Amy Cheuk Yin Lo)
#These authors contributed equally to this manuscript.

Funding: *This study was supported by Health and Medical Research Fund, the Food and Health Bureau, The Government of the Hong Kong Special Administrative Region (03142256); General Research Fund, Hong Kong Research Grants Council (GRF #HKU773613M); Seed Funding Programme for Basic Research (201811159123, 201910159191), The University of Hong Kong (all to ACYL).*
How to cite this article: *Lai AKW, Ng TC, Hung VKL, Tam KC, Cheung CW, Chung SK, Lo ACY (2022) Exacerbated VEGF up-regulation accompanies diabetes-aggravated hemorrhage in mice after experimental cerebral ischemia and delayed reperfusion. Neural Regen Res 17(7):1566-1575.*

Introduction

Diabetes mellitus is a prominent disease worldwide (Saeedi et al., 2019). Type 1 and type 2 diabetes increases the risk of ischemic stroke by 6.3-fold and 2.3-fold, respectively (Janghorbani et al., 2007), and one study reported that 31% of patients with ischemic stroke had diabetes (Reeves et al., 2010). Diabetic stroke is associated with a poor prognosis and high mortality (Eriksson et al., 2012; Lau et al., 2019).

The current standard intervention of large vessel occlusion is thrombolysis combined with endovascular thrombectomy (Shi et al., 2018). However, such reperfusion therapies are hindered by their narrow time window (for thrombolysis (alteplase): 4.5 hours after symptom onset; for endovascular thrombectomy: within 24 hours of last known normal to patients meeting DAWN trial eligibility criteria. DAWN excludes patients with baseline blood glucose > 400 mg/dL (22.2 mM), and for these patients, endovascular thrombectomy must be initiated within 6 hours of symptom onset; Jovin et al., 2017; Powers et al., 2019). In combination with a concern of increased intracranial hemorrhage risk in patients with diabetes/hyperglycemia (Celik et al., 2004) following reperfusion therapies (Reeves et al., 2010; Jiang et al., 2015), the rate of patients with diabetes receiving these beneficial treatments is lower than patients without diabetes (Reeves et al., 2010; Nathaniel et al., 2019; Saber et al., 2020).

Diabetic/hyperglycemic-exacerbated hemorrhage is likely to be the result of an aggravated inflammatory response primed by diabetic/hyperglycemic conditions (Jiang et al., 2021). Elevated serum matrix metallopeptidase 9 (MMP-9) has been associated with aggravated outcomes in clinical studies (Abdelnaseer et al., 2015; Zhong et al., 2017), as well as with cerebral hemorrhagic transformation in ischemia-reperfused animals (Elgebaly et al., 2010; McBride et al., 2020) and patients (Montaner et al., 2003). Furthermore, MMP-9 levels upon ischemic stroke has been found to be aggravated under hyperglycemic conditions in human serum (Setyopranoto et al., 2018) and in the cerebrums of diabetic mice (Kumari et al., 2011). Another matrix metallopeptidase, MMP-2, has also been considered to participate in the early stage of ischemic pathology (Yang and Rosenberg, 2015) and has found to be up-regulated very soon after experimental ischemia in baboons (Heo et al., 1999; Chang et al., 2003). MMP-2 has also been shown to destroy vascular integrity (Liu et al., 2012) and induce hemorrhagic transformation upon ischemia in mice (Lu et al., 2013). However, the mechanism/s underlying MMP-2/9 aggravation in diabetes upon ischemic stroke have not been well studied.

Although ischemic stroke has been investigated using hyperglycemic/diabetic animal models, most existing mice model studies induced either a short ischemia length (0.5–1.5 hours) or permanent occlusion in favor of reduced animal mortality (Tsuchiya et al., 2003; Villalba et al., 2018). These experimental paradigms have left the mechanism of diabetes-exacerbated outcomes under prolonged ischemia and delayed reperfusion largely unstudied. Thus, there is still limited progress in extending the window of reperfusion therapies for patients with diabetic stroke. However, a fast and complete reperfusion is important for outcome improvement in patients with stroke (Shi et al., 2018).

To fill this gap between basic research and the clinical situation, this study used *Ins2*$^{Akita/+}$ mice and 2-hour transient intraluminal MCAO to mimic delayed mechanical thrombectomy in patients with diabetic stroke, and investigated the causal mechanism of exacerbated intracerebral hemorrhage after prolonged ischemia in diabetes. *Ins2*$^{Akita/+}$ mice are a widely accepted model of type 1 diabetes (Lai and Lo, 2013) and have been used to study diabetic complications in various organ systems. The present results could aid the development of interventions to extend the treatment window of mechanical thrombectomy in patients with diabetic stroke by mitigating the exacerbated hemorrhage through the identification of suppression targets.

Materials and Methods

Animals

Twelve-week-old male *Ins2*$^{Akita/+}$ (n = 74; 23.7 ± 0.2 g) and *Ins2*$^{+/+}$ (n = 69; 25.3±0.2 g) mice were generated from C57BL/6-*Ins2*^{Akita}/J and C57BL/6J mice from Jackson Laboratory (Bar Harbor, ME, USA). They were kept under a 12-hour light/dark cycle and given *ad libitum* access to food and water. Two to five mice were housed per cage. Blood glucose level was measured using a glucometer (Ascensia Elite XL, Bayer Healthcare AG, Leverkusen, Germany).

The mice of both genotypes were randomly assigned to the sham or MCAO groups for each of the two time-points of assessment (2 hours ischemia/2 hours reperfusion or 2 hours ischemia/22 hours reperfusion), resulting in a total of eight groups (**Table 1**).

Experiments were conducted according to local and institute regulations and were approved by the Committee on the Use of Live Animals in Teaching and Research of the University of Hong Kong [CULATR 3834-15 (approval date January 5, 2016); 3977-16 (approval date April 13, 2016); and 4666-18 (approval date March 29, 2018)], as well as in compliance with the National Institutes of Health's Guide for the Care and Use of Laboratory Animals. This study was reported in accordance with the ARRIVE (Animal Research: Reporting of *In Vivo* Experiments) guidelines (Percie du Sert et al., 2020).

Induction of ischemia and reperfusion

Transient focal cerebral ischemia was induced using the intraluminal method (Lo et al., 2005; Li et al., 2012; Yang et al., 2012). In brief, mice were randomly assigned and were subjected to isoflurane (IsoFlo; 50019100, Zoetis Inc., Kalamazoo, MI, USA) inhalation anesthesia (2% isoflurane in 70% N_2O/30% O_2 for induction; 1.25% isoflurane in 70% N_2O/30% O_2 for maintenance). A filament coated with vinylpolysiloxane material (ESPE 7302, 3M Dental Products, St. Paul, MN, USA) was inserted into the right internal carotid artery and further advanced until reaching the middle cerebral artery. After 2 hours of ischemia, the filament was removed to commence reperfusion. Animals in the sham groups received the same procedures except for filament insertion. Relative cerebral blood flow in the middle cerebral artery territory was monitored by a laser Doppler flowmeter (Periflux 5000, Perimed AB, Järfälla, Sweden), with the reading at 5 minutes before ischemia set as 100%. Body temperature was maintained at 37 ± 0.5°C throughout the surgery. Mice were placed in an intensive care unit set at 30 ± 0.5°C during ischemia and for 4 hours after reperfusion commenced. Mice were sacrificed at either 2 hours (2 hours ischemia/2 hours reperfusion) or 22 hours (2 hours ischemia/22 hours reperfusion) of reperfusion (**Figure 1**).

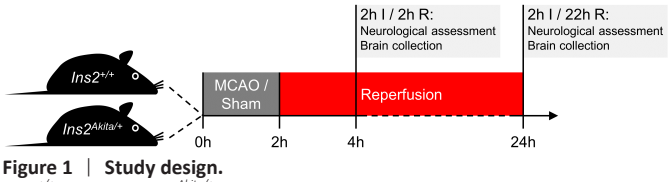

Figure 1 | **Study design.**
Ins2$^{+/+}$ mice and *Ins2*$^{Akita/+}$ mice were subjected to 2 hours of middle cerebral artery occlusion (MCAO) or sham surgery. Two hours later, the filament was removed to commence reperfusion in mice of the MCAO group, while mice in sham group received another sham surgery. At either 2 hours (2 h ischemia/2 h reperfusion; abbreviated as 2h I/2h R) or 22 hours (2 h ischemia/22 h reperfusion; abbreviated as 2h I/22h R) of reperfusion, mice were sacrificed for brain collection after neurological assessment.

Table 1 | **Number of experiments performed and body weight of mice used**

	Ins2$^{+/+}$ Sham	*Ins2*$^{Aktia/+}$ Sham	*Ins2*$^{+/+}$ MCAO	*Ins2*$^{Aktia/+}$ MCAO	*Ins2*$^{+/+}$ Sham	*Ins2*$^{Aktia/+}$ Sham	*Ins2*$^{+/+}$ MCAO	*Ins2*$^{Aktia/+}$ MCAO
	----------2h I / 2h R----------				----------2h I / 22h R----------			
Number of mice with experiment performed	10	9	24	21	10	10	25	34
Excluded due to incomplete occlusion/reperfusion	–	–	4	1	–	–	1	0
Included	10	9	20	20	10	10	24	34
Body weight before experiment (g)	25.3±0.5	24.1±0.4	26.0±0.4$^{\#}$	24.0±0.4^{++}	24.6±0.5	23.8±0.4	25.1±0.3	23.4±0.2^{++}

This table shows the number of mice used for each group. Mice were randomly drawn for the experiments. In mice with MCAO performed, relative cerebral blood flows were measured using a laser Doppler at 5 minutes before and during ischemia as well as 5 minutes after reperfusion, and animals were excluded from analysis if the measurements indicated any incomplete occlusion or reperfusion. In mice subjected to MCAO, the body weight of *Ins2*$^{Akita/+}$ mice were significantly lower than that of *Ins2*$^{+/+}$ mice. #P < 0.05, *vs.* *Ins2*$^{Akita/+}$ Sham; ++P < 0.01, *vs.* *Ins2*$^{+/+}$ MCAO; one-way analysis of variance followed by Tukey's HSD *post hoc* test; mean ± SEM. I: Ischemia; MCAO: middle cerebral artery occlusion; R: reperfusion.

Survival rate and neurological assessments

Experimental mice were closely monitored and survival rate was recorded. At the end of the reperfusion period (either 2 hours or 22 hours after reperfusion), neurological deficits were evaluated by an observer blinded to the genotype of the mouse (Lo et al., 2005; Li et al., 2012; Yang et al., 2012). The scoring system was as follows: 0 – no observable neurological deficits (normal); 1 – left wrist drop and walks straight (mild); 2 – left wrist drop and walks in a circular motion (moderate); 3 – loss of righting reflex (severe); and 4 – dead.

Tissue collection

Following decapitation under anesthesia with intraperitoneal injection of a mixture of ketamine (100 mg/kg, Alfasan International BV, Woerden, Netherlands) and xylazine (6 mg/kg, Alfasan International) at either 2 hours or 22 hours after reperfusion, mouse brains were cut into five 2 mm-thick coronal slices. For infarct and histological analyses, brain slices were stained with 2% 2,3,5-triphenyltetrazolium chloride and fixed in 10% formalin (see below). For molecular analyses, infarct and penumbra areas of brain slice number two to four were collected at 1 mm away from the midline, snap-frozen in liquid nitrogen and homogenized together in 10 mM phosphate buffered saline (PBS), pH 7.4, containing protease inhibitors (4693159001, Roche Applied Science) and phosphatase inhibitors (524628, Merck KGaA, Darmstadt, Germany), followed by protein or mRNA extraction (see below).

Measurement of infarct, swelling, and hemorrhagic transformation

Freshly cut brain slices were stained with 2% 2,3,5-triphenyltetrazolium chloride (TTC; T8877, Sigma-Aldrich, St. Louis, MO, USA) in PBS at 37°C for 7.5 minutes and then fixed overnight in 10% buffered formalin (Merck KGaA). The red live and white infarct areas on the posterior side of brain slices were measured using SigmaScan Pro (SPSS Inc., Chicago, IL, USA) by a researcher who was blinded to the genotypes of each mouse. Infarct areas and volume were estimated indirectly to minimize inaccuracy due to swelling (Swanson et al., 1990), and hemispheric swelling was estimated using the following equation: (ipsilateral volume − contralateral volume)/contralateral volume × 100%. Hemorrhagic transformations, identified as dark-brown areas on the posterior side of brain slice number three (at approximately bregma –0.34 mm), were presented as percentages of infarct and contralateral areas.

Histochemistry and immunohistochemistry

To further verify the presence of hemorrhage, the fixed brain slices were embedded in paraffin (T565, Fisher Chemical, Thermo Fisher Scientific, Waltham, MA, USA) and cut into sections of 7 μm thickness using a microtome (HM 315R, Microm International GmbH, Walldorf, Germany). Sections were mounted onto positive-charged glass slides and dried overnight in an oven set to 37°C, deparaffinized at 57°C for 30 minutes, followed by soaking in toluene twice for 5 minutes each, and rehydrated through a graded series of ethanol. After over-staining with Harris's hematoxylin for 5 minutes, the sections were differentiated in acid alcohol for a few seconds followed by bluing in Scott's tap and staining in 1% aqueous eosin for 3 minutes. Subsequently, the sections were dehydrated in ascending ethanol gradients followed by toluene for 3 times for 5 minutes each, mounted with Permount (SP15-500, Fisher Chemical) and covered with cover slips. Microscopic photos of infarct cores were taken using a light microscope (Eclipse 80i; Nikon, Tokyo, Japan) equipped with a digital camera (SPOT RT3 25.4 2 Mp Slider; Diagnostic Instruments, Inc., Sterling Heights, MI, USA), and patches of orange red indicated the presence of hemorrhage.

Western blot analysis

Lysates of infarct and penumbra areas of brain slices two to four were mixed with 2× ice-cold radioimmunoprecipitation assay lysis buffer in a 1:1 ratio. Supernatants were collected following centrifugation at 16,100 × *g* and 4°C for 30 minutes, mixed with Laemmli reducing loading dye at 95°C for 5 minutes, separated by SDS-PAGE at 30 mA (4% stacking gel and 10% separating gel, 10 μg protein per lane), and transferred onto polyvinylidene fluoride membranes (IPVH00010, Merck KGaA) at 300 mA for 2 hours on ice. The membranes were blocked with 5% skimmed milk (Nestlé S.A., Switzerland) in Tris-buffered saline with 0.1% Tween 20 detergent (0.1% TBST) and incubated with primary antibodies (**Additional Table 1**) diluted with 5% bovine serum albumin (USB Corporation, Affymetrix, Santa Clara, CA, USA) in 0.1% TBST at 4°C overnight followed by peroxide-conjugated anti-rabbit IgG (PI-1000, 1:2000, Vector Laboratories, Burlingame, CA, USA) or anti-mouse IgG (PI-2000, 1:5000, Vector Laboratories) secondary antibodies at room temperature for 1 hour. Immunoreactivities were detected using enhanced chemiluminescence reagents (RPN2106, GE Healthcare, Buckinghamshire, UK or K-12042-D10, Advansta, CA, USA) and light-sensitive films (47410 19291, Fujifilm, Tokyo, Japan), quantified using ImageJ (U.S. National Institutes of Health, Bethesda, MD, USA), and normalized using an endogenous protein (actin or α-tubulin), except for phospho (p)-Akt, p-Erk1/2, and p-p38 MAPK, which were normalized with their respective total expressions.

Real-time PCR analysis

After mixing lysates of infarct and penumbra areas of brain slices two to four with ice-cold RNAiso plus (9109, Takara Bio Inc., Japan) at a ratio of 1:4, total RNA was extracted by the phenol:chloroform extraction method, and cDNA was prepared from 2 μg of the extracted RNA (SuperScript VILO; 11754050, Life Technologies, USA), both according to the manufacturers' instructions. Real-time PCR reactions were performed using the StepOnePlus system and SYBR Green technology (4385610, Life Technologies) with the primers listed in **Additional Table 2**. The relative mRNA expression levels were shown as fold changes to the *Ins2*$^{+/+}$ sham group after normalizing with the endogenous gene *β-actin*, following the manufacturer's protocol.

Statistical analysis

No statistical methods were used to predetermine sample sizes; however, the sample sizes of this study (~20 animals in each group) were similar to those reported in our previous publication (Li et al., 2012). The total number of mice used in each group is shown in **Table 1**. Data are expressed as the mean ± standard error of mean (SEM) and statistical tests were performed using GraphPad Prism (v5.02; GraphPad Software, Inc., USA). Survival rate and the neurological score were analyzed using the log-rank test and Mann-Whitney *U* test, respectively. All other measurements were analyzed using a one-way analysis of variance followed by Tukey's HSD *post hoc* tests or unpaired Student's *t*-tests, except for the comparison of hemorrhagic transformation areas, in which case the Mann-Whitney *U* test was used due to non-normality of the data. A *P*-value of < 0.05 was considered statistically significant.

Results

Physiological parameters of *Ins2*$^{+/+}$ and *Ins2*$^{Akita/+}$ mice

Ins2$^{Akita/+}$ mice displayed hyperglycemia from 4 weeks of age and a decreased body weight from 13 weeks of age (**Figure 2**). *Ins2*$^{Akita/+}$ mice had higher relative cerebral blood flow during ischemia, which was similar in both genotypes during reperfusion (**Table 2**).

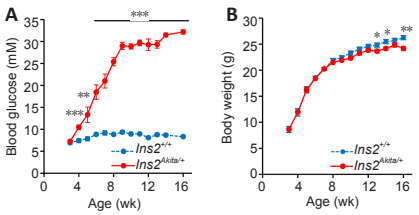

Figure 2 | *Ins2*$^{Akita/+}$ mice displayed hyperglycemia and decreased body weight.

Ins2$^{Akita/+}$ mice displayed hyperglycemia (A) and decreased body weight (B) from 4 and 13 weeks of age, respectively, when compared with *Ins2*$^{+/+}$ mice (*n* = 10–19; **P* < 0.05, ***P* < 0.01, and ****P* < 0.001, unpaired Student's *t*-test; mean ± SEM).

Table 2 | Physiological conditions of *Ins2*$^{Akita/+}$ mice and their wildtype littermates before and after ischemia

	Ins2$^{+/+}$ MCAO	*Ins2*$^{Aktia/+}$ MCAO	*Ins2*$^{+/+}$ MCAO	*Ins2*$^{Aktia/+}$ MCAO
	----------2h I / 2h R-------		--------2h I / 22h R--------	
N number	20	20	24	34
Relative cerebral blood flow (%)				
5 min before ischemia	100	100	100	100
During ischemia	11.0±1.3	14.4±1.4	11.7±1.1	15.0±1.1*
5 min after reperfusion	102.2±10.6	118.4±8.8	120.7±11.0	108.5±8.9
Body temperature (°C)				
At ischemia	36.9±0.0	36.9±0.0	36.8±0.0	36.8±0.0
At reperfusion	36.9±0.1	37.0±0.0	36.9±0.0	36.9±0.0

Relative cerebral blood flows were measured using a laser Doppler at 5 minutes before and during ischemia as well as 5 minutes after reperfusion. The reading of relative blood flow at 5 minutes before ischemia was set as 100%, and the sequential changes of blood flow were calculated as a reference to this. Relative cerebral blood flows were similar in both *Ins2*$^{Akita/+}$ and *Ins2*$^{+/+}$ mice after reperfusion, but they were faster in *Ins2*$^{Akita/+}$ mice during ischemia. **P* < 0.05, *vs.* *Ins2*$^{+/+}$ MCAO at 22 h R (22 hours after reperfusion), unpaired Student's *t*-test. Data are expressed as the mean ± SEM. I: Ischemia; MCAO: middle cerebral artery occlusion; R: reperfusion.

Ins2$^{Akita/+}$ mice subjected to prolonged ischemia showed decreased survival rate and worse neurological outcomes

Ins2$^{Akita/+}$ mice had a significantly lower survival rate than *Ins2*$^{+/+}$ mice after reperfusion (**Figure 3A** and **B**). The majority of lethality was observed in the first 4 hours after reperfusion in *Ins2*$^{Akita/+}$ mice, while death of *Ins2*$^{+/+}$ mice mostly occurred later. Moreover, *Ins2*$^{Akita/+}$ mice suffered from more severe neurological deficits at 2 hours after reperfusion (**Figure 3C**), whereas there was no between-group difference at 22 hours after reperfusion (**Figure 3D**).

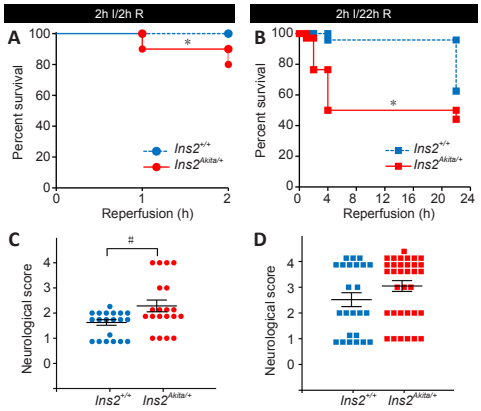

Figure 3 | More severe neurological deficits and lower survival rate in *Ins2*$^{Akita/+}$ mice after 2 hours of MCAO.

(A & B) Survival rate after 2 hours of ischemia recorded at various time points after reperfusion. The majority of deaths of *Ins2*$^{Akita/+}$ mice occurred before 4 hours of reperfusion. (C & D) Neurological deficits were graded from 0 to 4 at the end of the assigned period of reperfusion. A significantly higher neurological score was observed in *Ins2*$^{Akita/+}$ mice compared with *Ins2*$^{+/+}$ mice at 2 hours after reperfusion, but the difference diminished at 22 hours after reperfusion (2h I/2h R: *Ins2*$^{+/+}$ (*n* = 20), *Ins2*$^{Akita/+}$ (*n* = 20); 2h I/22h R: *Ins2*$^{+/+}$ (*n* = 24), *Ins2*$^{Akita/+}$ (*n* = 34); **P* < 0.05, Log-rank (Mantel-Cox) test; #*P* < 0.05, Mann-Whitney *U* test; mean ± SEM).

Ins2$^{Akita/+}$ mice displayed accelerated infarct development and increased hemorrhage after prolonged ischemia

Figure 4A and **B** show posterior photographs of TTC-stained brain slices at 2 and 22 hours after reperfusion, respectively. At 2 hours after reperfusion, infarct areas were significantly larger in brain slices one to three of *Ins2*$^{Akita/+}$ brains compared with *Ins2*$^{+/+}$ brains (**Figure 4C**), with significantly larger infarct volume compared with *Ins2*$^{+/+}$ brains and a trend towards greater hemispheric swelling (**Figure 4E** and **F**). However, these differences between *Ins2*$^{+/+}$ and *Ins2*$^{Akita/+}$ mice diminished at 22 hours after reperfusion (**Figure 4D**, **G**, and **H**).

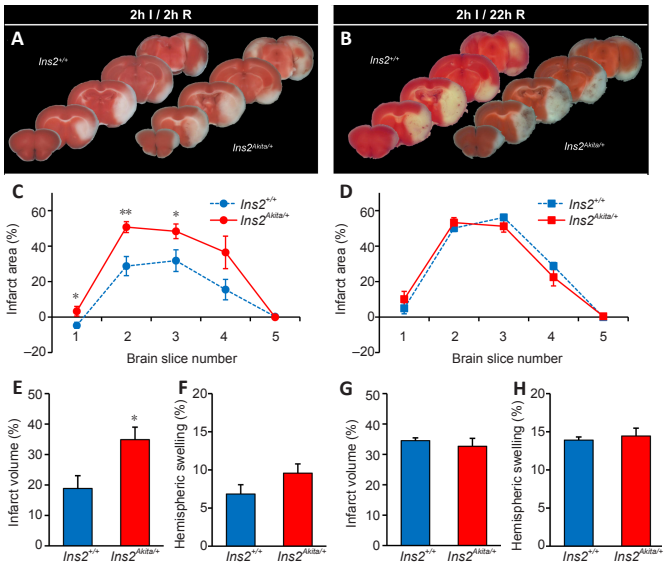

Figure 4 | Increased development rate of infarct area and infarct volume upon 2h I/2h R ischemic challenge in *Ins2*$^{Akita/+}$ mice.

Representative TTC-stained brain slices of mice after 2h I/2h R (A) and 2h I/22h R (B). Calculated infarct area, infarct volume, and hemispheric swelling after 2h I/2h R are shown in C, E, and F; those after 2h I/22h R are shown in D, G, and H, respectively. 2h I/2h R: *Ins2*$^{+/+}$ middle cerebral artery occlusion (MCAO) (*n* = 12), *Ins2*$^{Akita/+}$ MCAO (*n* = 10), 2h I/22h R: *Ins2*$^{+/+}$ MCAO (*n* = 10), *Ins2*$^{Akita/+}$ MCAO (*n* = 10); **P* < 0.05, ***P* < 0.01, unpaired Student's *t*-test; mean ± SEM. I: Ischemia; R: reperfusion; TTC: 2,3,5-triphenyltetrazolium chloride.

Hemorrhage (red-pink spreading) was observed in ipsilateral *Ins2*$^{Akita/+}$ brains as early as 2 hours after reperfusion (**Figure 5A** and **B**), while eosin staining revealed its presence around blood vessels in both the infarct core (**Figure 5C–F**) and penumbra area (data not shown). Quantitative analysis revealed a significantly larger hemorrhagic area in brain slice number three of *Ins2*$^{Akita/+}$ mice at 2 hours after reperfusion (**Figure 5G** and **H**), which was robustly exacerbated at 22 hours after reperfusion (**Figure 5I** and **J**).

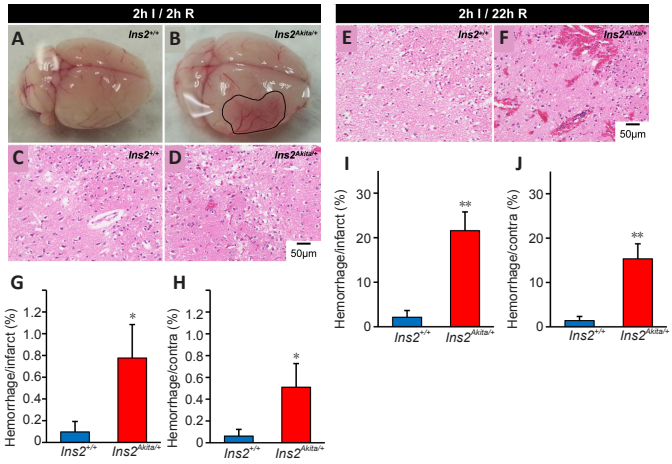

Figure 5 | Increased hemorrhage in *Ins2*$^{Akita/+}$ mice as early as 2 hours after reperfusion following 2 hours of ischemia, which was further advanced at 22 hours after reperfusion.

General view of the ipsilateral side of the brain of *Ins2*$^{+/+}$ (A) and *Ins2*$^{Akita/+}$ (B) mice after 2h I/2h R challenge. The black line outlining the reddish area indicates the presence of hemorrhage. Representative regions of the infarct core located in the cerebral cortex after 2 hours (C & D) and 22 hours (E & F) of reperfusion are shown. Sections were stained with hematoxylin and eosin, with which red blood cells were stained in an orange-red color. Scale bars: 50 μm. Quantification of the hemorrhagic area was presented as a ratio of the infarct core as well as a ratio of the contralateral side in brain slice number three of mice after 2 hours (G & H) and 22 hours (I & J) of reperfusion. **P* < 0.05, ***P* < 0.01, Mann-Whitney *U* test; mean ± SEM). I: Ischemia; R: reperfusion.

Decreased tight junction protein ZO-1 level and increased blood-brain barrier-disrupting MMP expressions in *Ins2*$^{Akita/+}$ brains after prolonged ischemia

Infarct and penumbra areas of operated mice were subjected to Western blot analysis. At 2 hours after reperfusion, there was a reduced level of tight junction protein ZO-1 in operated *Ins2*$^{+/+}$ mice upon MCAO, which was further exaggerated in *Ins2*$^{Akita/+}$ mice (**Figure 6A**). Likewise, at 22 hours after reperfusion, only *Ins2*$^{Akita/+}$ mice showed a significant reduction in ZO-1 level (**Figure 6B**).

Western blot analysis of MMP-2, which is known to disrupt the blood-brain barrier following stroke, was significantly up-regulated only in *Ins2*$^{Akita/+}$ ipsilateral brains at 2 hours after reperfusion (**Figure 6C**). Interestingly, at 22 hours after reperfusion, the previously up-regulated MMP-2 expression in *Ins2*$^{Akita/+}$ mice returned to a normal level that was similar to that of sham-operated controls; however, MMP-2 expression in *Ins2*$^{+/+}$ mice was significantly up-regulated (**Figure 6D**).

The expression of MMP-9 was also significantly increased in *Ins2*$^{Akita/+}$ mouse brains at 2 hours after reperfusion when compared with that of the sham-operated *Ins2*$^{+/+}$ mice (**Figure 6E**), but not at 22 hours after reperfusion (**Figure 6F**).

Up-regulation of vascular endothelial growth factor and its downstream factors p-Erk1/2 and p-p38 MAPK, but not p-Akt in *Ins2*$^{Akita/+}$ brains after prolonged ischemia

At 2 hours after reperfusion, vascular endothelial growth factor (VEGF) and p-Erk1/2 were remarkably over-expressed in *Ins2*$^{Akita/+}$ ipsilateral brains when compared with *Ins2*$^{+/+}$ mice (**Figure 7A** and **C**). The expression of p-p38 mitogen-activated protein kinase (p-p38 MAPK) was also significantly higher in *Ins2*$^{Akita/+}$ ipsilateral brains than that of sham-operated *Ins2*$^{+/+}$ controls (**Figure 7E**). In contrast, there were no significant changes in p-Akt level in operated mice of both genotypes when compared with levels of sham-operated mice (**Figure 7G**).

Similarly, at 22 hours after reperfusion, VEGF expression only remarkably increased in *Ins2*$^{Akita/+}$ mice (**Figure 7B**). While there was a significant increase of p-Erk1/2 expression in the ipsilateral brains of both genotypes, its level in *Ins2*$^{Akita/+}$ mouse brains was significantly higher than that of *Ins2*$^{+/+}$ mice (**Figure 7D**). The expression of p-p38 in both genotypes was also significantly higher than that of the sham-operated controls (**Figure 7F**). No significant differences in p-Akt level were found between any of the groups (**Figure 7H**).

Increased endoplasmic reticulum stress markers expression in *Ins2*$^{Akita/+}$ brains during the early stage of reperfusion

The expression of endoplasmic reticulum (ER) stress markers in ipsilateral brains was revealed by RT-PCR. *CHOP* was significantly up-regulated in both *Ins2*$^{+/+}$ and *Ins2*$^{Akita/+}$ brains at 2 hours after reperfusion, with a more pronounced increase in *Ins2*$^{Akita/+}$ mice (**Figure 8A**). In contrast, a significant increase in *BiP* expression was only found in *Ins2*$^{Akita/+}$ mice when compared with sham-operated *Ins2*$^{+/+}$ controls (**Figure 8A**). These increases vanished at 22 hours after reperfusion (**Figure 8B**).

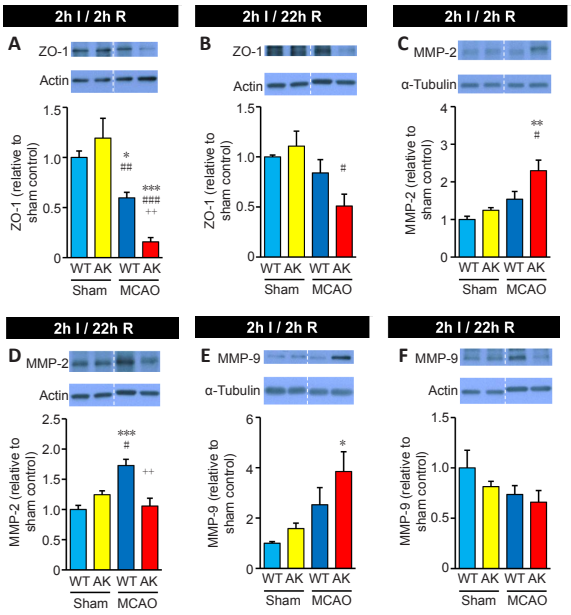

Figure 6 | Vulnerable blood vessel integrity in *Ins2*$^{Akita/+}$ mice at 2 hours and 22 hours after reperfusion following 2 hours of ischemia.

Protein expressions of ZO-1, MMP-2, and MMP-9 for the two experimental groups, 2h I/2h R (A, C, & E) and 2h I/22h R (B, D & F), were semi-quantified using Western blot analysis. The corresponding fold changes of these proteins are shown in the bottom panel. WT: *Ins2*$^{+/+}$, AK: *Ins2*$^{Akita/+}$; A, C, & E: *Ins2*$^{+/+}$ Sham: *n* = 4, *Ins2*$^{Akita/+}$ Sham: *n* = 4, *Ins2*$^{+/+}$ 2h R: *n* = 5, *Ins2*$^{Akita/+}$ 2h R: *n* = 7; B, D, & F: *Ins2*$^{+/+}$ Sham: *n* = 4, *Ins2*$^{Akita/+}$ Sham: *n* = 4, *Ins2*$^{+/+}$ 22h R: *n* = 5, *Ins2*$^{Akita/+}$22h R: *n* = 5; **P* < 0.05, ***P* < 0.01, and ****P* < 0.001, *vs. Ins2*$^{+/+}$ Sham; #*P* < 0.05, ##*P* < 0.01, and ###*P* < 0.001, *vs. Ins2*$^{Akita/+}$ Sham; ++*P* < 0.01, *vs. Ins2*$^{+/+}$ 2h R or *Ins2*$^{+/+}$ 22h R; one-way analysis of variance followed by Tukey's HSD *post hoc* test; mean ± SEM. I: Ischemia; MCAO: middle cerebral artery occlusion; MMP: matrix metallopeptidase; R: reperfusion.

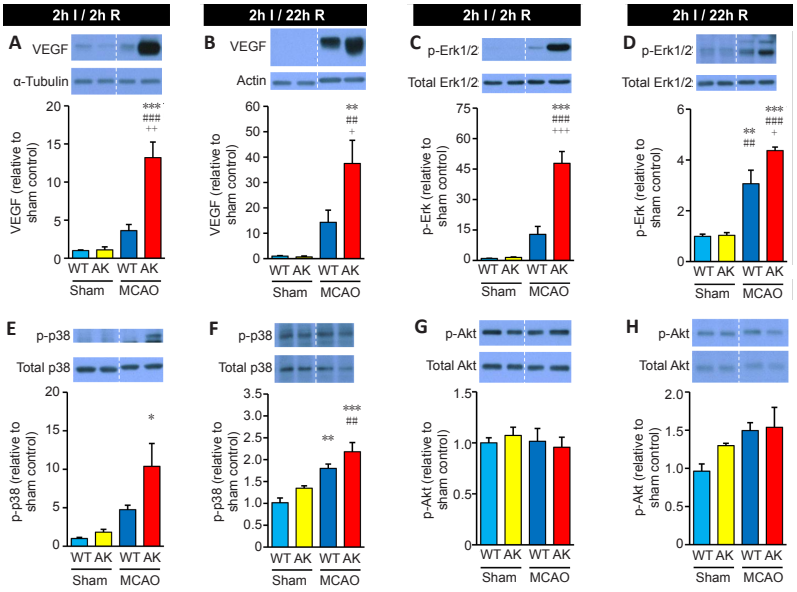

Figure 7 | Up-regulation of VEGF and its endothelium destabilizing downstream factors in *Ins2*$^{Akita/+}$ mice at 2 hours and 22 hours after reperfusion following 2 hours of ischemia.

Protein expressions of VEGF, p-Erk1/2, p-p38, and p-Akt for the two experimental groups, 2h I/2h R (A, C, E, and G) and 2h I/22h R (B, D, F, and H), were semi-quantitated using Western blot analysis. The corresponding fold changes of these proteins are shown in the bottom panel. (WT: *Ins2*$^{+/+}$, AK: *Ins2*$^{Akita/+}$; A, C, E, and G: *Ins2*$^{+/+}$ Sham: $n = 4$, *Ins2*$^{Akita/+}$ Sham: $n = 4$, *Ins2*$^{+/+}$ 2h R: $n = 5$, *Ins2*$^{Akita/+}$ 2h R: $n = 7$; B, D, F, and H: *Ins2*$^{+/+}$ Sham: $n = 4$, *Ins2*$^{Akita/+}$ Sham: $n = 4$, *Ins2*$^{+/+}$ 22h R: $n = 5$, *Ins2*$^{Akita/+}$ 22h R: $n = 5$; $^{*}P < 0.05$, $^{**}P < 0.01$, and $^{***}P < 0.001$, *vs.* *Ins2*$^{+/+}$ Sham; $^{\#\#}P < 0.01$, and $^{\#\#\#}P < 0.001$, *vs.* *Ins2*$^{Akita/+}$ Sham; $^{+}P < 0.05$, $^{++}P < 0.01$, and $^{+++}P < 0.001$, *vs.* *Ins2*$^{+/+}$ 2h R or *Ins2*$^{+/+}$ 22h R; one-way analysis of variance followed by Tukey's HSD *post hoc* test; mean ± SEM). I: Ischemia; MCAO: middle cerebral artery occlusion; R: reperfusion; VEGF: vascular endothelial growth factor.

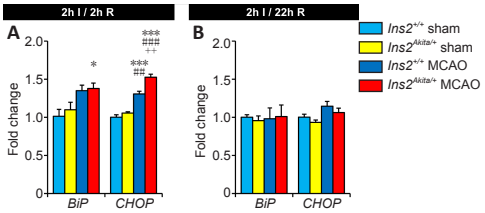

Figure 8 | *CHOP*, which is involved in the ER stress pathway, was further increased in the *Ins2*$^{Akita/+}$ mice after 2 hours of reperfusion following 2 hours of ischemia.

mRNA expressions of ER stress-targets were analyzed after 2 hours of ischemic challenge followed by 2 hours (A) or 22 hours (B) of reperfusion. (A: *Ins2*$^{+/+}$ Sham: $n = 4$, *Ins2*$^{Akita/+}$ Sham: $n = 4$, *Ins2*$^{+/+}$ 2h R: $n = 5$, *Ins2*$^{Akita/+}$ 2h R: $n = 7$; B: *Ins2*$^{+/+}$ Sham: $n = 4$, *Ins2*$^{Akita/+}$ Sham: $n = 4$, *Ins2*$^{+/+}$ 22h R: $n = 5$, *Ins2*$^{Akita/+}$ 22h R: $n = 5$; $^{*}P < 0.05$ and $^{***}P < 0.001$, *vs.* *Ins2*$^{+/+}$ Sham; $^{\#\#}P < 0.01$ and $^{\#\#\#}P < 0.001$, *vs.* *Ins2*$^{Akita/+}$ Sham; $^{++}P < 0.01$, *vs.* *Ins2*$^{+/+}$ 2h R; one-way analysis of variance followed by Tukey's HSD *post hoc* test; mean ± SEM). ER: Endoplasmic reticulum; I: ischemia; MCAO: middle cerebral artery occlusion; R: reperfusion.

Discussion

In the current study, we demonstrated that induction of prolonged ischemia followed by reperfusion in diabetic *Ins2*$^{Akita/+}$ mice could mimic the exacerbated outcomes observed in patients with diabetes upon ischemic stroke but with delayed reperfusion. Multiple studies have reported more severe neurological deficits, larger infarcts, and hemorrhagic transformation in diabetic animals after experimental stroke (Toung et al., 2000; Kusaka et al., 2004; Elgebaly et al., 2010; Chen et al., 2011; Ye et al., 2011; Cui et al., 2012; Ning et al., 2012; Yan et al., 2012; Liao et al., 2014; Mishiro et al., 2014). After inducing 2-hour long ischemia, we found early mortality and hemorrhagic transformation in diabetic *Ins2*$^{Akita/+}$ mice at as early as 2 hours after reperfusion, with a robust increase in hemorrhagic transformation at 22 hours after reperfusion. This study revealed that the diabetes-exacerbated hemorrhagic transformation was due to a quicker and heavier compromise of blood vessel integrity, which was shown by the greater loss of tight junction protein ZO-1 from 2 hours of reperfusion in *Ins2*$^{Akita/+}$ mice. Furthermore, this rapid compromise of blood vessel integrity was associated with accelerated VEGF and p-Erk1/2 up-regulation in *Ins2*$^{Akita/+}$ mice, which suggests that VEGF is a potential target for attenuating aggravated hemorrhage following delayed reperfusion in diabetic stroke.

MMP-2, which can destroy vascular integrity (Liu et al., 2012) and induce hemorrhagic transformation upon ischemia in mice (Lu et al., 2013), has been found to be up-regulated very soon after MCAO in baboons (Heo et al., 1999; Chang et al., 2003). Furthermore, MMP-9 has been associated with hemorrhagic transformation following ischemia in multiple animal and clinical studies (Montaner et al., 2003; del Zoppo, 2010; Elgebaly et al., 2010; Khatri et al., 2012; McBride et al., 2020). In the current study, we observed a premature increase of MMP-2 in *Ins2*$^{Akita/+}$ mice at 2 hours after reperfusion compared with *Ins2*$^{+/+}$ mice, in which the increase was only evident at 22 hours after reperfusion. We also observed a potentially higher MMP-9 expression in *Ins2*$^{Akita/+}$ mice at 2 hours after reperfusion, yet this difference was not significant, which may be due to the limited sample size. Together with a greater decline in ZO-1 levels starting at 2 hours after reperfusion, these results indicate that early increased expressions of MMPs in diabetic animals after experimental stroke result in a quicker and more severe compromise of blood vessel integrity and therefore hemorrhagic transformation, which may account for the worse outcomes and earlier mortality in *Ins2*$^{Akita/+}$ mice.

Up-regulation of VEGF has been reported in murine models of transient MCAO starting from 1 hour after reperfusion and persisting for at least 1 day (Hayashi et al., 1997; Shimamura et al., 2006; Yao et al., 2010; Wu et al., 2014), but its role in exacerbating diabetic ischemic stroke has not been well studied. We observed a remarkable and persistent VEGF up-regulation during reperfusion in *Ins2*$^{Akita/+}$ mice, which suggests that diabetic conditions play a role in magnifying VEGF over-expression after prolonged ischemia. The deleterious role of VEGF reported in rodents after stroke includes increasing infarct volume, blood-brain barrier breakdown, and hemorrhagic transformation (Zhang et al., 2000; Kaya et al., 2005). Meanwhile, antagonism of VEGF signaling has been found to significantly reduce brain swelling in both normal adult (van Bruggen et al., 1999) and diabetic mice (Kim et al., 2018) at 1 day after reperfusion. In parallel with worse neurological deficits, earlier mortality, increased hemorrhagic transformation, and blood-brain barrier breakdown, as demonstrated by ZO-1 down-regulation in *Ins2*$^{Akita/+}$ mice, the current study further substantiated the deleterious role of VEGF in exacerbating diabetic ischemic stroke during reperfusion.

Erk1/2 and p38 MAPK are two downstream factors of the VEGF pathway that are responsible for the proliferation and migration of endothelial cells during angiogenesis, respectively, while Akt is another downstream factor

promoting endothelial cell survival and vasodilation (Kowanetz and Ferrara, 2006; Melincovici et al., 2018). Inhibiting the MEK-Erk1/2 pathway reduced MMP-9 up-regulation in the middle cerebral artery upon MCAO in rats (Maddahi et al., 2009), while inhibiting p38 activation attenuated hypoxia-induced brain vascular hyperpermeability in mice (Clauss et al., 2001; Issbrucker et al., 2003). At 2 hours after reperfusion, while there was no significant change in the level of p-Akt, we detected significant increases in p-Erk1/2 and p-p38 MAPK expressions in diabetic *Ins2*$^{Akita/+}$ mice only. These persisted at high levels at 22 hours after reperfusion, at which point the expressions in *Ins2*$^{+/+}$ mice also increased, but to a lesser extent. These results suggest that the rapidly exaggerated VEGF expression found in diabetic *Ins2*$^{Akita/+}$ mice triggered an earlier and stronger activation of its downstream factors Erk1/2 and p38; this likely caused premature angiogenesis that started immediately after reperfusion instead of 12–24 hours following ischemic insults in normoglycemic rodents and 3–4 days in humans (Beck and Plate, 2009). Therefore, diabetes-aggravated VEGF expression is likely to be responsible for the exaggerated hemorrhagic transformation observed in patients with diabetes during reperfusion after ischemia.

Other than prompting angiogenesis, VEGF, Erk1/2, and p38 MAPK are pro-inflammatory factors that might also aggravate I/R injury via triggering inflammation (del Zoppo, 2009; Hong et al., 2019). VEGF can induce activation and proliferation of microglia (Mosher et al., 2012) and promote recruitment of neutrophils and monocytes/macrophages (Cursiefen et al., 2004; Sinnathamby et al., 2015). Its downstream players, Erk1/2 and p38 MAPK, also trigger inflammation cascades leading to the production of various cytokines and inflammatory responses (Hommes et al., 2003; Kaminska, 2005; Arthur and Ley, 2013). Importantly, Erk1/2- and p38 MAPK-triggered inflammatory cytokines have been linked to aggravation of cerebral I/R injury (Barone et al., 2001; Wang et al., 2004; Maddahi and Edvinsson, 2010). During the acute phase of stroke, uncontrolled and excess inflammation is a major contributor to tissue damage (del Zoppo, 2009; Hong et al., 2019) and is exacerbated under diabetic conditions (Tureyen et al., 2011). Therefore, the early increase in VEGF, p-Erk1/2, and p-p38 MAPK found in *Ins2*$^{Akita/+}$ mice is also suggestive of a diabetes-triggered robust inflammation during reperfusion in response to prolonged ischemia, which, in addition to premature angiogenesis discussed above, could explain the early deteriorating outcomes in diabetes. This should be investigated in future studies.

ER stress has been found to participate in the pathology of I/R injury (Nakka et al., 2010; Xin et al., 2014; Rastogi and Srivastava, 2019; Thiebaut et al., 2019), and inhibiting ER stress could attenuate I/R injury in diabetic rats (Srinivasan and Sharma, 2011a, 2012; Bai et al., 2021). The current study investigated BiP (GRP78) and CHOP, two unfolded protein response (UPR) markers known to alter mRNA levels during ischemia/reperfusion of various tissues (Bilecová-Rabajdová et al., 2010; Li et al., 2014; Noh et al., 2015). BiP is a pro-survival UPR chaperone, while CHOP plays a major role in ER stress-mediated apoptosis, is a major cause of I/R-induced neuronal cell death, and has been linked to more severe ischemic stroke outcomes (Xin et al., 2014; Rastogi and Srivastava, 2019). At 2 hours of reperfusion after prolonged ischemia, while there was similar non-significant increase in mRNA levels of *BiP* in both genotypes, *CHOP* expression was higher in diabetic *Ins2*$^{Akita/+}$ mice when compared with normoglycemic *Ins2*$^{+/+}$ mice. This indicates that diabetic conditions aggravated ER stress, as observed in the diabetic rat brain (Srinivasan and Sharma, 2011b), heart (Li et al., 2020), and kidney (Zhang et al., 2020) upon I/R injury, and rapidly shifted the BiP-driven pro-survival UPR to CHOP-driven pro-apoptotic UPR (Xin et al., 2014; Nakka et al., 2016; Rastogi and Srivastava, 2019) at 2 hours after reperfusion. Alternatively, the chronic inflammation and higher oxidative stress environment (Liu et al., 2015; Levard et al., 2021) in diabetes may deposit an excess CHOP up-regulation upon I/R injury, although the possible effect of inflammation on ER stress and UTR warrants further investigations (Hotamisligil, 2010; Hasnain et al., 2012).

Given the close link between hypoxia, ER stress, and inflammation (Hotamisligil, 2010; Hasnain et al., 2012; Ramakrishnan et al., 2014; Levard et al., 2021), it is likely that ER stress and CHOP are involved in inducing VEGF expression. Excess ER stress causes an accumulation of reactive oxygen species (ROS) (Malhotra and Kaufman, 2007; Zeeshan et al., 2016), which induces VEGF expression (Kim and Byzova, 2014). Furthermore, CHOP has been found to escalate ROS production during ER stress by both inducing ERO1α expression and resuming protein synthesis (Malhotra and Kaufman, 2007; Nakka et al., 2016). Alternatively, CHOP has been suggested to induce VEGF expression by potentiating the HIF-1α-VEGF pathway as *ATF4*-siRNA (Pereira et al., 2014) (ATF4 is a transcription regulator of CHOP) and *CHOP*-siRNA has been found to suppress VEGF transcription *in vitro* (Hu et al., 2017). Therefore, it is likely that the aggravated *CHOP* expression is responsible for the rapidly increased VEGF expression found in diabetic *Ins2*$^{Akita/+}$ mice, which resulted in extensive hemorrhagic transformation and probably exacerbated other outcomes upon prolonged ischemia and reperfusion.

Limitations

Although this study postulates the relationship between diabetes-exacerbated hemorrhagic transformation and aggravated VEGF up-regulation during delayed reperfusion, the potential of suppressing the VEGF pathway in attenuating diabetes-exacerbated stroke outcomes was not explored in the present study due to the high mortality of mice following prolonged ischemia. In addition, neurological score was used as a measurement of neurological deficit in this study. Although carried out in a blinded manner, the subjective nature of the assessment could intrinsically bring inaccuracy. More objective methods for assessing neurological deficit, such as the adhesive removal test, should be included in future research.

Conclusion

We demonstrated that diabetic conditions might play a key role in the rapid exacerbation of hemorrhage transformation at the reperfusion phase following prolonged ischemia. We postulate that this rapid exacerbation seen under diabetic, but not normoglycemic conditions, is at least partially underpinned by diabetes-aggravated premature VEGF up-regulation shortly after reperfusion. This has deleterious effects via rapid triggering of vascular disintegration and, hence, hemorrhagic transformation, and this premature VEGF aggravation is associated with diabetes-enhanced *CHOP* expression.

Exacerbated hemorrhage is a major concern in patients with diabetes/hyperglycemia (Celik et al., 2004) following reperfusion therapies (Reeves et al., 2010; Jiang et al., 2015). This adverse effect contributes to the contraindication of reperfusion therapy in patients with diabetes beyond the therapeutic window. By considering the relationship between aggravated VEGF up-regulation and hemorrhage, this study suggests a potential strategy of using VEGF antagonists in mitigating exacerbated hemorrhage in patients with diabetic stroke following delayed reperfusion therapy. The administration of VEGF antagonists, such as bevacizumab and sunitinib, before reperfusion therapy could attenuate VEGF-induced premature vascular disintegration, thus limiting hemorrhagic transformation and extending the therapeutic window of reperfusion therapy in patients with diabetic stroke

for a better clinical outcome. In future research, the effect of VEGF antagonism during delayed reperfusion in diabetic animals should be explored by the use of VEGF antagonists like bevacizumab and sunitinib.

Author contributions: *Study design: AKWL; literature search, manuscript preparation: AKWL, TCN; experimental studies and data acquisition: AKWL, VKLH, KCT; data analysis: AKWL, TCN, VKLH; manuscript editing and review: TCN, CWC, SKC, ACYL; study concept and design, literature search, experimental studies, data analysis, guarantor: ACYL. All authors approved the final version of the manuscript.*
Conflicts of interest: *None declared.*
Editor note: ACYL is an Editorial Board member of Neural Regeneration Research. She was blinded from reviewing or making decisions on the manuscript. The article was subject to the journal's standard procedures, with peer review handled independently of this Editorial Board member and their research groups.
Financial support: *This study was supported by Health and Medical Research Fund, the Food and Health Bureau, The Government of the Hong Kong Special Administrative Region (03142256); General Research Fund, Hong Kong Research Grants Council (GRF #HKU773613M); Seed Funding Programme for Basic Research (201811159123, 201910159191), The University of Hong Kong (all to ACYL).*
Institutional review board statement: *The animal experiments were approved by the Committee on the Use of Live Animals in Teaching and Research of the University of Hong Kong [CULATR 3834-15 (approval date January 5, 2016); 3977-16 (approval date April 13, 2016); and 4666-18 (approval date March 29, 2018)].*
Author statement: *The abstract has been presented at Neuroscience 2016 (San Diego, CA, USA; Nov 12-16, 2016), 14th International Symposium on Healthy Aging (Hong Kong SAR, China; March 16–17, 2019), and Neuroscience 2019 (Chicago, IL, USA; October 19–23, 2019), respectively.*

Data sharing statement: *Datasets analyzed during the current study are available from the corresponding author on reasonable request.*
Plagiarism check: *Checked twice by iThenticate.*
Peer review: *Externally peer reviewed.*

Additional files:
Additional Table 1: *Antibodies used in Western blot analysis.*
Additional Table 2: *Primer sequences used in real-time PCR analysis.*
Additional Figure 1: *Original blot images for Figure 6.*
Additional Figure 2: *Original blot images for Figure 7.*

References

Abdelnaseer M, Elfayomi N, Hassan E, Kamal M, Hamdy A, Elsawy E (2015) Serum matrix metalloproteinase-9 in acute ischemic stroke and its relation to stroke severity. Egypt J Neurol Psychiatr Neurosurg 52:274-278.

Arthur JS, Ley SC (2013) Mitogen-activated protein kinases in innate immunity. Nat Rev Immunol 13:679-692.

Bai B, Li D, Xue G, Feng P, Wang M, Han Y, Wang Y, Hölscher C (2021) The novel GLP-1/GIP dual agonist DA3-CH is more effective than liraglutide in reducing endoplasmic reticulum stress in diabetic rats with cerebral ischemia-reperfusion injury. Nutr Metabo Cardiovasc Dis 31:333-343.

Barone FC, Irving EA, Ray AM, Lee JC, Kassis S, Kumar S, Badger AM, Legos JJ, Erhardt JA, Ohlstein EH, Hunter AJ, Harrison DC, Philpott K, Smith BR, Adams JL, Parsons AA (2001) Inhibition of p38 mitogen-activated protein kinase provides neuroprotection in cerebral focal ischemia. Med Res Rev 21:129-145.

Beck H, Plate KH (2009) Angiogenesis after cerebral ischemia. Acta Neuropathol 117:481-496.

Bilecová-Rabajdová M, Urban P, Mašlanková J, Veselá J, Mareková M (2010) Analysis of changes in pro (Gadd153) and anti apoptotic (Grp78) gene expression after ischemic-reperfusion injury of the small intestine. Prague Med Rep 111:249-256.

Celik Y, Utku U, Asil T, Balci K (2004) Factors affecting haemorrhagic transformation in middle cerebral artery infarctions. J Clin Neurosci 11:656-658.

Chang DI, Hosomi N, Lucero J, Heo JH, Abumiya T, Mazar AP, del Zoppo GJ (2003) Activation systems for latent matrix metalloproteinase-2 are upregulated immediately after focal cerebral ischemia. J Cereb Blood Flow Metab 23:1408-1419.

Chen J, Ye X, Yan T, Zhang C, Yang XP, Cui X, Cui Y, Zacharek A, Roberts C, Liu X, Dai X, Lu M, Chopp M (2011) Adverse effects of bone marrow stromal cell treatment of stroke in diabetic rats. Stroke 42:3551-3558.

Clauss M, Sunderkotter C, Sveinbjornsson B, Hippenstiel S, Willuweit A, Marino M, Haas E, Seljelid R, Scheurich P, Suttorp N, Grell M, Risau W (2001) A permissive role for tumor necrosis factor in vascular endothelial growth factor-induced vascular permeability. Blood 97:1321-1329.

Cui H, Lee JH, Kim JY, Koo BN, Lee JE (2012) The neuroprotective effect of agmatine after focal cerebral ischemia in diabetic rats. J Neurosurg Anesthesiol 24:39-50.

Cursiefen C, Chen L, Borges LP, Jackson D, Cao J, Radziejewski C, D'Amore PA, Dana MR, Wiegand SJ, Streilein JW (2004) VEGF-A stimulates lymphangiogenesis and hemangiogenesis in inflammatory neovascularization via macrophage recruitment. J Clin Invest 113:1040-1050.

del Zoppo GJ (2009) Inflammation and the neurovascular unit in the setting of focal cerebral ischemia. Neuroscience 158:972-982.

del Zoppo GJ (2010) The neurovascular unit, matrix proteases, and innate inflammation. Ann N Y Acad Sci 1207:46-49.

Elgebaly MM, Prakash R, Li W, Ogbi S, Johnson MH, Mezzetti EM, Fagan SC, Ergul A (2010) Vascular protection in diabetic stroke: role of matrix metalloprotease-dependent vascular remodeling. J Cereb Blood Flow Metab 30:1928-1938.

Eriksson M, Carlberg B, Eliasson M (2012) The disparity in long-term survival after a first stroke in patients with and without diabetes persists: the Northern Sweden MONICA study. Cerebrovasc Dis 34:153-160.

Hasnain SZ, Lourie R, Das I, Chen AC, McGuckin MA (2012) The interplay between endoplasmic reticulum stress and inflammation. Immunol Cell Biol 90:260-270.

Hayashi T, Abe K, Suzuki H, Itoyama Y (1997) Rapid induction of vascular endothelial growth factor gene expression after transient middle cerebral artery occlusion in rats. Stroke 28:2039-2044.

Heo JH, Lucero J, Abumiya T, Koziol JA, Copeland BR, del Zoppo GJ (1999) Matrix metalloproteinases increase very early during experimental focal cerebral ischemia. J Cereb Blood Flow Metab 19:624-633.

Hommes DW, Peppelenbosch MP, van Deventer SJ (2003) Mitogen activated protein (MAP) kinase signal transduction pathways and novel anti-inflammatory targets. Gut 52:144-151.

Hong P, Gu RN, Li FX, Xiong XX, Liang WB, You ZJ, Zhang HF (2019) NLRP3 inflammasome as a potential treatment in ischemic stroke concomitant with diabetes. J Neuroinflammation 16:121.

Hotamisligil GS (2010) Endoplasmic reticulum stress and the inflammatory basis of metabolic disease. Cell 140:900-917.

Hu Y, Lu X, Xu Y, Lu L, Yu S, Cheng Q, Yang B, Tsui CK, Ye D, Huang J, Liang X (2017) Salubrinal attenuated retinal neovascularization by inhibiting CHOP-HIF1α-VEGF pathways. Oncotarget 8:77219-77232.

Issbrucker K, Marti HH, Hippenstiel S, Springmann G, Voswinckel R, Gaumann A, Breier G, Drexler HC, Suttorp N, Clauss M (2003) p38 MAP kinase--a molecular switch between VEGF-induced angiogenesis and vascular hyperpermeability. FASEB J 17:262-264.

Janghorbani M, Hu FB, Willett WC, Li TY, Manson JE, Logroscino G, Rexrode KM (2007) Prospective study of type 1 and type 2 diabetes and risk of stroke subtypes: the Nurses' Health Study. Diabetes Care 30:1730-1735.

Jiang S, Fei A, Peng Y, Zhang J, Lu YR, Wang HR, Chen M, Pan S (2015) Predictors of outcome and hemorrhage in patients undergoing endovascular therapy with solitaire stent for acute ischemic stroke. PLoS One 10:e0144452.

Jiang Y, Liu N, Han J, Li Y, Spencer P, Vodovoz SJ, Ning MM, Bix G, Katakam PVG, Dumont AS, Wang X (2021) Diabetes mellitus/poststroke hyperglycemia: a detrimental factor for tPA thrombolytic stroke therapy. Transl Stroke Res 12:416-427.

Jovin TG, Saver JL, Ribo M, Pereira V, Furlan A, Bonafe A, Baxter B, Gupta R, Lopes D, Jansen O, Smith W, Gress D, Hetts S, Lewis RJ, Shields R, Berry SM, Graves TL, Malisch T, Rai A, Sheth KN, et al. (2017) Diffusion-weighted imaging or computerized tomography perfusion assessment with clinical mismatch in the triage of wake up and late presenting strokes undergoing neurointervention with Trevo (DAWN) trial methods. Int J Stroke 12:641-652.

Kaminska B (2005) MAPK signalling pathways as molecular targets for anti-inflammatory therapy--from molecular mechanisms to therapeutic benefits. Biochim Biophys Acta 1754:253-262.

Kaya D, Gursoy-Ozdemir Y, Yemisci M, Tuncer N, Aktan S, Dalkara T (2005) VEGF protects brain against focal ischemia without increasing blood--brain permeability when administered intracerebroventricularly. J Cereb Blood Flow Metab 25:1111-1118.

Khatri R, McKinney AM, Swenson B, Janardhan V (2012) Blood-brain barrier, reperfusion injury, and hemorrhagic transformation in acute ischemic stroke. Neurology 79:S52-57.

Kim E, Yang J, Park KW, Cho S (2018) Inhibition of VEGF signaling reduces diabetes-exacerbated brain swelling, but not infarct size, in large cerebral infarction in mice. Transl Stroke Res 9:540-548.

Kim YW, Byzova TV (2014) Oxidative stress in angiogenesis and vascular disease. Blood 123:625-631.

Kowanetz M, Ferrara N (2006) Vascular endothelial growth factor signaling pathways: therapeutic perspective. Clin Cancer Res 12:5018-5022.

Kumari R, Willing LB, Patel SD, Baskerville KA, Simpson IA (2011) Increased cerebral matrix metalloprotease-9 activity is associated with compromised recovery in the diabetic db/db mouse following a stroke. J Neurochem 119:1029-1040.

Kusaka I, Kusaka G, Zhou C, Ishikawa M, Nanda A, Granger DN, Zhang JH, Tang J (2004) Role of AT1 receptors and NAD(P)H oxidase in diabetes-aggravated ischemic brain injury. Am J Physiol Heart Circ Physiol 286:H2442-2451.

Lai AK, Lo AC (2013) Animal models of diabetic retinopathy: summary and comparison. J Diabetes Res 2013:106594.

Lau LH, Lew J, Borschmann K, Thijs V, Ekinci EI (2019) Prevalence of diabetes and its effects on stroke outcomes: A meta-analysis and literature review. J Diabetes Investig 10:780-792.

Levard D, Buendia I, Lanquetin A, Glavan M, Vivien D, Rubio M (2021) Filling the gaps on stroke research: Focus on inflammation and immunity. Brain Behav Immun 91:649-667.

Li H, Zhu X, Fang F, Jiang D, Tang L (2014) Down-regulation of GRP78 enhances apoptosis via CHOP pathway in retinal ischemia-reperfusion injury. Neurosci Lett 575:68-73.

Li SY, Yang D, Fu ZJ, Woo T, Wong D, Lo AC (2012) Lutein enhances survival and reduces neuronal damage in a mouse model of ischemic stroke. Neurobiol Dis 45:624-632.

Li W, Li W, Leng Y, Xiong Y, Xia Z (2020) Ferroptosis is involved in diabetes myocardial ischemia/reperfusion injury through endoplasmic reticulum stress. DNA Cell Biol 39:210-225.

Liao J, Ye Z, Huang G, Xu C, Guo Q, Wang E (2014) Delayed treatment with NSC23766 in streptozotocin-induced diabetic rats ameliorates post-ischemic neuronal apoptosis through suppression of mitochondrial p53 translocation. Neuropharmacology 85:508-516.

Liu H, Cao MM, Wang Y, Li LC, Zhu LB, Xie GY, Li YB (2015) Endoplasmic reticulum stress is involved in the connection between inflammation and autophagy in type 2 diabetes. Gen Comp Endocrinol 210:124-129.

Liu J, Jin X, Liu KJ, Liu W (2012) Matrix metalloproteinase-2-mediated occludin degradation and caveolin-1-mediated claudin-5 redistribution contribute to blood-brain barrier damage in early ischemic stroke stage. J Neurosci 32:3044-3057.

Lo AC, Chen AY, Hung VK, Yaw LP, Fung MK, Ho MC, Tsang MC, Chung SS, Chung SK (2005) Endothelin-1 overexpression leads to further water accumulation and brain edema after middle cerebral artery occlusion via aquaporin 4 expression in astrocytic end-feet. J Cereb Blood Flow Metab 25:998-1011.

Lu A, Suofu Y, Guan F, Broderick JP, Wagner KR, Clark JF (2013) Matrix metalloproteinase-2 deletions protect against hemorrhagic transformation after 1 h of cerebral ischemia and 23 h of reperfusion. Neuroscience 253:361-367.

Maddahi A, Edvinsson L (2010) Cerebral ischemia induces microvascular pro-inflammatory cytokine expression via the MEK/ERK pathway. J Neuroinflammation 7:14.

Maddahi A, Chen Q, Edvinsson L (2009) Enhanced cerebrovascular expression of matrix metalloproteinase-9 and tissue inhibitor of metalloproteinase-1 via the MEK/ERK pathway during cerebral ischemia in the rat. BMC Neurosci 10:56.

Malhotra JD, Kaufman RJ (2007) Endoplasmic reticulum stress and oxidative stress: a vicious cycle or a double-edged sword? Antioxid Redox Signal 9:2277-2293.

McBride DW, Gren ECK, Kelln W, Hayes WK, Zhang JH (2020) Crotalus atrox disintegrin reduces hemorrhagic transformation by attenuating matrix metalloproteinase-9 activity after middle cerebral artery occlusion in hyperglycemic male rats. J Neurosci Res 98:191-200.

Melincovici CS, Boşca AB, Şuşman S, Mărginean M, Mihu C, Istrate M, Moldovan IM, Roman AL, Mihu CM (2018) Vascular endothelial growth factor (VEGF)- key factor in normal and pathological angiogenesis. Rom J Morphol Embryol 59:455-467.

Mishiro K, Imai T, Sugitani S, Kitashoji A, Suzuki Y, Takagi T, Chen H, Oumi Y, Tsuruma K, Shimazawa M, Hara H (2014) Diabetes mellitus aggravates hemorrhagic transformation after ischemic stroke via mitochondrial defects leading to endothelial apoptosis. PLoS One 9:e103818.

Montaner J, Molina CA, Monasterio J, Abilleira S, Arenillas JF, Ribó M, Quintana M, Alvarez-Sabín J (2003) Matrix metalloproteinase-9 pretreatment level predicts intracranial hemorrhagic complications after thrombolysis in human stroke. Circulation 107:598-603.

Mosher KI, Andres RH, Fukuhara T, Bieri G, Hasegawa-Moriyama M, He Y, Guzman R, Wyss-Coray T (2012) Neural progenitor cells regulate microglia functions and activity. Nat Neurosci 15:1485-1487.

Nakka VP, Gusain A, Raghubir R (2010) Endoplasmic reticulum stress plays critical role in brain damage after cerebral ischemia/reperfusion in rats. Neurotox Res 17:189-202.

Nakka VP, Prakash-Babu P, Vemuganti R (2016) Crosstalk between endoplasmic reticulum stress, oxidative stress, and autophagy: potential therapeutic targets for acute CNS injuries. Mol Neurobiol 53:532-544.

Nathaniel TI, Ubah C, Wormack L, Gainey J (2019) The telestroke and thrombolysis therapy in diabetic stroke patients. Diabetol Metab Syndr 11:36.

Ning R, Chopp M, Yan T, Zacharek A, Zhang C, Roberts C, Cui X, Lu M, Chen J (2012) Tissue plasminogen activator treatment of stroke in type-1 diabetes rats. Neuroscience 222:326-332.

Noh MR, Kim JI, Han SJ, Lee TJ, Park KM (2015) C/EBP homologous protein (CHOP) gene deficiency attenuates renal ischemia/reperfusion injury in mice. Biochim Biophys Acta 1852:1895-1901.

Percie du Sert N, Ahluwalia A, Alam S, Avey MT, Baker M, Browne WJ, Clark A, Cuthill IC, Dirnagl U, Emerson M, Garner P, Holgate ST, Howells DW, Hurst V, Karp NA, Lazic SE, Lidster K, MacCallum CJ, Macleod M, Pearl EJ, et al. (2020) Reporting animal research: Explanation and elaboration for the ARRIVE guidelines 2.0. PLoS Biol 18:e3000411.

Pereira ER, Frudd K, Awad W, Hendershot LM (2014) Endoplasmic reticulum (ER) stress and hypoxia response pathways interact to potentiate hypoxia-inducible factor 1 (HIF-1) transcriptional activity on targets like vascular endothelial growth factor (VEGF). J Biol Chem 289:3352-3364.

Powers WJ, Rabinstein AA, Ackerson T, Adeoye OM, Bambakidis NC, Becker K, Biller J, Brown M, Demaerschalk BM, Hoh B, Jauch EC, Kidwell CS, Leslie-Mazwi TM, Ovbiagele B, Scott PA, Sheth KN, Southerland AM, Summers DV, Tirschwell DL (2019) Guidelines for the Early Management of Patients With Acute Ischemic Stroke: 2019 Update to the 2018 Guidelines for the Early Management of Acute Ischemic Stroke: A Guideline for Healthcare Professionals From the American Heart Association/American Stroke Association. Stroke 50:e344-418.

Ramakrishnan S, Anand V, Roy S (2014) Vascular endothelial growth factor signaling in hypoxia and inflammation. J Neuroimmune Pharmacol 9:142-160.

Rastogi N, Srivastava VK (2019) Ischemic stroke-induced endoplasmic reticulum stress. In: Advancement in the pathophysiology of cerebral stroke (Patnaik R, Tripathi AK, Dwivedi A, eds), pp 43-57. Singapore: Springer Singapore.

Reeves MJ, Vaidya RS, Fonarow GC, Liang L, Smith EE, Matulonis R, Olson DM, Schwamm LH (2010) Quality of care and outcomes in patients with diabetes hospitalized with ischemic stroke: findings from Get With the Guidelines-Stroke. Stroke 41:e409-417.

Saber H, Khatibi K, Szeder V, Tateshima S, Colby GP, Nour M, Jahan R, Duckwiler G, Liebeskind DS, Saver JL (2020) Reperfusion therapy frequency and outcomes in mild ischemic stroke in the United States. Stroke 51:3241-3249.

Saeedi P, Petersohn I, Salpea P, Malanda B, Karuranga S, Unwin N, Colagiuri S, Guariguata L, Motala AA, Ogurtsova K, Shaw JE, Bright D, Williams R (2019) Global and regional diabetes prevalence estimates for 2019 and projections for 2030 and 2045: Results from the International Diabetes Federation Diabetes Atlas, 9(th) edition. Diabetes Res Clin Pract 157:107843.

Setyopranoto I, Malueka RG, Panggabean AS, Widyadharma IPE, Sadewa AH, Lamsudin R, Wibowo S (2018) Association between Increased matrix metalloproteinase-9 (MMP-9) levels with hyperglycaemia incidence in acute ischemic stroke patients. Open Access Maced J Med Sci 6:2067-2072.

Shi L, Rocha M, Leak RK, Zhao J, Bhatia TN, Mu H, Wei Z, Yu F, Weiner SL, Ma F, Jovin TG, Chen J (2018) A new era for stroke therapy: Integrating neurovascular protection with optimal reperfusion. J Cereb Blood Flow Metab 38:2073-2091.

Shimamura N, Matchett G, Yatsushige H, Calvert JW, Ohkuma H, Zhang J (2006) Inhibition of integrin alphavbeta3 ameliorates focal cerebral ischemic damage in the rat middle cerebral artery occlusion model. Stroke 37:1902-1909.

Sinnathamby T, Yun J, Clavet-Lanthier M, Cheong C, Sirois MG (2015) VEGF and angiopoietins promote inflammatory cell recruitment and mature blood vessel formation in murine sponge/Matrigel model. J Cell Biochem 116:45-57.

Srinivasan K, Sharma SS (2011a) Sodium phenylbutyrate ameliorates focal cerebral ischemic/reperfusion injury associated with comorbid type 2 diabetes by reducing endoplasmic reticulum stress and DNA fragmentation. Behav Brain Res 225:110-116.

Srinivasan K, Sharma SS (2011b) Augmentation of endoplasmic reticulum stress in cerebral ischemia/reperfusion injury associated with comorbid type 2 diabetes. Neurol Res 33:858-865.

Srinivasan K, Sharma SS (2012) 3-Bromo-7-nitroindazole attenuates brain ischemic injury in diabetic stroke via inhibition of endoplasmic reticulum stress pathway involving CHOP. Life Sci 90:154-160.

Swanson RA, Morton MT, Tsao-Wu G, Savalos RA, Davidson C, Sharp FR (1990) A semiautomated method for measuring brain infarct volume. J Cereb Blood Flow Metab 10:290-293.

Thiebaut AM, Hedou E, Marciniak SJ, Vivien D, Roussel BD (2019) Proteostasis during cerebral ischemia. Front Neurosci 13:637.

Toung TK, Hurn PD, Traystman RJ, Sieber FE (2000) Estrogen decreases infarct size after temporary focal ischemia in a genetic model of type 1 diabetes mellitus. Stroke 31:2701-2706.

Tsuchiya D, Hong S, Kayama T, Panter SS, Weinstein PR (2003) Effect of suture size and carotid clip application upon blood flow and infarct volume after permanent and temporary middle cerebral artery occlusion in mice. Brain Res 970:131-139.

Tureyen K, Bowen K, Liang J, Dempsey RJ, Vemuganti R (2011) Exacerbated brain damage, edema and inflammation in type-2 diabetic mice subjected to focal ischemia. J Neurochem 116:499-507.

van Bruggen N, Thibodeaux H, Palmer JT, Lee WP, Fu L, Cairns B, Tumas D, Gerlai R, Williams SP, van Lookeren Campagne M, Ferrara N (1999) VEGF antagonism reduces edema formation and tissue damage after ischemia/reperfusion injury in the mouse brain. J Clin Invest 104:1613-1620.

Villalba H, Shah K, Albekairi TH, Sifat AE, Vaidya B, Abbruscato TJ (2018) Potential role of myo-inositol to improve ischemic stroke outcome in diabetic mouse. Brain Res 1699:166-176.

Wang ZQ, Wu DC, Huang FP, Yang GY (2004) Inhibition of MEK/ERK 1/2 pathway reduces pro-inflammatory cytokine interleukin-1 expression in focal cerebral ischemia. Brain Res 996:55-66.

Wu Y, Wang L, Dai C, Ma G, Zhang Y, Zhang X, Wu Z (2014) Neuroprotection by platelet-activating factor acetylhydrolase in a mouse model of transient cerebral ischemia. Neurosci Lett 558:26-30.

Xin Q, Ji B, Cheng B, Wang C, Liu H, Chen X, Chen J, Bai B (2014) Endoplasmic reticulum stress in cerebral ischemia. Neurochem Int 68:18-27.

Yan T, Chopp M, Ye X, Liu Z, Zacharek A, Cui Y, Roberts C, Buller B, Chen J (2012) Niaspan increases axonal remodeling after stroke in type 1 diabetes rats. Neurobiol Dis 46:157-164.

Yang D, Li SY, Yeung CM, Chang RC, So KF, Wong D, Lo AC (2012) Lycium barbarum extracts protect the brain from blood-brain barrier disruption and cerebral edema in experimental stroke. PLoS One 7:e33596.

Yang Y, Rosenberg GA (2015) Matrix metalloproteinases as therapeutic targets for stroke. Brain Res 1623:30-38.

Yao X, Miao W, Li M, Wang M, Ma J, Wang Y, Miao L, Feng H (2010) Protective effect of albumin on VEGF and brain edema in acute ischemia in rats. Neurosci Lett 472:179-183.

Ye X, Chopp M, Cui X, Zacharek A, Cui Y, Yan T, Shehadah A, Roberts C, Liu X, Lu M, Chen J (2011) Niaspan enhances vascular remodeling after stroke in type 1 diabetic rats. Exp Neurol 232:299-308.

Zeeshan HM, Lee GH, Kim HR, Chae HJ (2016) Endoplasmic reticulum stress and associated ROS. Int J Mol Sci 17:327.

Zhang J, Wang L, Gong D, Yang Y, Liu X, Chen Z (2020) Inhibition of the SIRT1 signaling pathway exacerbates endoplasmic reticulum stress induced by renal ischemia/reperfusion injury in type 1 diabetic rats. Mol Med Rep 21:695-704.

Zhang ZG, Zhang L, Jiang Q, Zhang R, Davies K, Powers C, Bruggen N, Chopp M (2000) VEGF enhances angiogenesis and promotes blood-brain barrier leakage in the ischemic brain. J Clin Invest 106:829-838.

Zhong C, Yang J, Xu T, Xu T, Peng Y, Wang A, Wang J, Peng H, Li Q, Ju Z, Geng D, Zhang Y, He J (2017) Serum matrix metalloproteinase-9 levels and prognosis of acute ischemic stroke. Neurology 89:805-812.

C-Editors: Zhao M, Li CH; T-Editor: Jia Y

Additional Table 1 Antibodies used in Western blot analysis

Target	Dilution	Cat#	Supplier
α-Tubulin	1:20000	sc-5286	Santa Cruz Biotechnology, Santa Cruz, CA
Actin	1:5000	MAB1501	Merck KGaA, Darmstadt, Germany
MMP-2	1:1000	4022	Cell Signaling Technologies, MA
MMP-9	1:1000	2270	Cell Signaling Technologies, MA
ZO-1	1:1000	40-2300	Zymed Laboratories, South San Francisco, CA
VEGF	1:1000	sc-7269	Santa Cruz Biotechnology, Santa Cruz, CA
Total Akt	1:1000	9272	Cell Signaling Technologies, MA
p-Akt	1:1500	9277	Cell Signaling Technologies, MA
Total Erk1/2	1:2000	9107	Cell Signaling Technologies, MA
p-Erk1/2	1:2000	9106	Cell Signaling Technologies, MA
Total p38 MAPK	1:1000	9212	Cell Signaling Technologies, MA
p-p38 MAPK	1:1000	9211	Cell Signaling Technologies, MA

MAPK: Mitogen-activated protein kinase; MMP: matrix metallopeptidase; VEGF: vascular endothelial growth factor.

Additional Table 2 Primer sequences used in real-time PCR analysis

Target	Primer sequence (5' to 3')	Reference
β-actin	Forward: GACGGCCAGGTCATCACTATTG	Binet et al., 2013
	Reverse: CCACAGGATTCCATACCCAAGA	
BiP	Forward: AAGGTGAACGACCCCTAACAAA	Binet et al., 2013
	Reverse: GTCACTCGGAGAATACCATTAACATCT	
CHOP	Forward: GTTGAAGATGAGCGGGTGGCAGC	Wang et al., 2012
	Reverse: GCACGTGGACCAGGTTCTGCTT	

Binet F, Mawambo G, Sitaras N, Tetreault N, Lapalme E, Favret S, Cerani A, Leboeuf D, Tremblay S, Rezende F, Juan AM, Stahl A, Joyal JS, Milot E, Kaufman RJ, Guimond M, Kennedy TE, Sapieha P (2013) Neuronal ER stress impedes myeloid-cell-induced vascular regeneration through IRE1α degradation of netrin-1. Cell Metab 17:353-371.

Wang Z, Wang H, Xu ZM, Ji YL, Chen YH, Zhang ZH, Zhang C, Meng XH, Zhao M, Xu DX (2012) Cadmium-induced teratogenicity: association with ROS-mediated endoplasmic reticulum stress in placenta. Toxicol Appl Pharmacol 259:236-247.